

## Clear Sky Radiance (CSR) product derived from Himawari-8 data

IMAI Takahito\* and UESAWA Daisaku\*\*

### Abstract

The Meteorological Satellite Center (MSC) has developed a Clear Sky Radiance (CSR) product using data from Himawari-8's Advanced Himawari Imager (AHI). The product, which has been supplied to operational numerical weather prediction (NWP) centers since 7 July 2015, provides data on area-averaged brightness temperatures for clear pixels. Cloudy pixels can be regarded as clear when the contribution of cloud top emission to the total radiance is negligible (e.g., in cases of low cloud for water vapor bands). In CSR calculation, such cloudy pixels are regarded as clear in addition to regular clear pixels. Accordingly, clear pixel ratios differ for each AHI band because atmospheric transmittance depends on the band. CSR is determined for each 16 x 16 infrared pixel segment, which corresponds to a resolution of 32 x 32 km<sup>2</sup> at the sub-satellite point. The product will be assimilated into NWP models.

### 1. Introduction

The Clear Sky Radiance (CSR) product provides data on area-averaged radiances and/or brightness temperatures for clear pixels, and is assimilated into numerical weather prediction (NWP) models. For operational NWP centers, CSR products from geostationary meteorological satellite data are indispensable, as are atmospheric motion vectors (AMVs) derived by tracking cloud features in successive images.

The Meteorological Satellite Center (MSC) of the Japan Meteorological Agency (JMA) has provided CSR products derived from MTSAT (Multifunctional Transport Satellite) units since 2006 (Uesawa 2009). Its current CSR product is made using data from Himawari-8, which is Japan's new-generation geostationary meteorological satellite. The Himawari-8 CSR product was launched on 7 July 2015.

This paper describes the Himawari-8 CSR product. The algorithm is outlined in Section 3.

### 2. Himawari-8

Himawari-8 is the world's first next-generation geostationary meteorological satellite (Bessho et al. 2016). It was launched on 7 October 2014 and has been operational since 7 July 2015. The unit took over East Asia and Western Pacific observation previously conducted for more than three decades by five GMS (Geostationary Meteorological Satellite) units and two satellites from the MTSAT series.

Himawari-8 carries the Advanced Himawari Imager (AHI), which has 16 bands (See Table 1 for AHI specifications). Himawari-8/AHI performs full-disk observations at 10-minute intervals, and observes the Japan area and specific target areas at 2.5-minute intervals. The Himawari-8 CSR product is derived from full-disk observations.

---

\*Office of Observation Systems Operation, Observation Department, Japan Meteorological Agency

\*\*System Engineering Division, Data Processing Department, Meteorological Satellite Center

(Received August 28, 2015, Accepted November 6, 2015)

**Table 1. Himawari-8 AHI specifications**

	Band #	Central wavelength ( $\mu\text{m}$ )	Spatial resolution (km)
Visible	#1	0.47	1
	#2	0.51	
	#3	0.64	0.5
Near-Infrared	#4	0.86	1
	#5	1.6	2
	#6	2.3	
Infrared	#7	3.9	
	#8	6.2	
	#9	6.9	
	#10	7.3	
	#11	8.6	
	#12	9.6	
	#13	10.4	
	#14	11.2	
#15	12.4		
#16	13.3		

### 3. Algorithm

#### 3.1. Overview

The processing of the algorithm is as outlined below. A flowchart of the processing is shown in Figure 1.

- Step 1 (input data collection): CSR product processing involves use of data listed below. All data files are stored in a 5,500 x 5,500 infrared pixel array.
  - Brightness temperature (bands 7 – 16)
  - Satellite/Solar zenith angles
  - Atmospheric transmittances (for bands 7 – 16) based on radiative transfer calculation (see Section 3.2)
  - Cloud mask and cloud top pressure from the fundamental cloud product (Imai and Yoshida 2016, Mouri et al. 2016)
- Step 2 (CSR calculation): All input data are segmented into a 16 x 16-pixel array, which corresponds to a resolution of 32 x 32 km<sup>2</sup> at the sub-satellite point. For each segment, CSR is calculated as the average brightness temperature of clear pixels for bands 7 – 16 (see Section 3.2). The location (latitude/longitude) of CSR data is given as

the center of the segment (rather than as the centers of clear pixels, which differ by band). However, this may not be the optimal representative location when there are few clear pixels that are at the edge of the segment. Spatial coverage extends to satellite zenith angles of 65° from the sub-satellite point.

- Step 3 (BUFR encoding): The CSR product is encoded in Binary Universal Form for data Representation (BUFR). The data descriptor is [3 10 23] (see WMO BUFR Table D; available online at [www.wmo.int/pages/prog/www/WMOCodes.html](http://www.wmo.int/pages/prog/www/WMOCodes.html)). In order to reduce file size, CSR data are divided into several BUFR files each containing up to 8,000 data points. For the same reason, only clear sky brightness temperature data are stored in BUFR files; clear sky spectral radiance data are not.

#### 3.2. CSR calculation

The concept of Himawari-8 CSR calculation is similar to that of the MSG SEVIRI CSR (water vapor 6.2  $\mu\text{m}$  channel) product (EUMETSAT 2014), in which low-cloud pixels are considered clear. If only regular clear pixels (i.e., those with no cloud at any altitude) were used in CSR calculation, atmospheric information from cloudy pixels would be discarded in moist conditions where water vapor band radiances emitted from low cloud tops may not reach the top of the atmosphere (TOA). However, it is desirable to retain as much information as possible about the atmosphere (particularly water vapor) for NWP assimilation. For optimal provision of data on radiance emitted from the atmosphere (but not from cloud), the approach described below is adopted for CSR calculation.

Regular clear pixels in the fundamental cloud product (cloud mask; Imai and Yoshida 2016) are naturally regarded as clear in CSR calculation. For AHI bands with strong absorption (e.g., water vapor bands), cloudy pixels in the fundamental cloud product can also be regarded as clear when the contribution of cloud top emission to the total radiance is negligible (e.g., in cases characterized by low cloud). In CSR calculation, such cloudy pixels are regarded as clear in addition to regular

clear pixels.

Atmospheric transmittance from the cloud top pressure level to TOA ( $\tau(p_c)$ , where  $p_c$  represents cloud top pressure) is interpolated from the transmittance profile  $\tau(p)$  (where  $p$  represents pressure levels). If  $\tau(p_c)$  is less than a particular threshold value (0.0001), cloudy pixels are treated as clear in CSR calculation (Fig. 2). As atmospheric transmittance depends on the band, judgment of whether a cloudy pixel can be regarded as clear varies by band (Fig. 3). Cloud top pressure is retrieved in the fundamental cloud product (Mouri et al. 2016). Atmospheric transmittance profiles are calculated using the RTTOV v11.1 fast radiative transfer model (Eyre 1991; Saunders et al. 1999; Matricardi et al. 2004). Atmospheric profiles (temperature and water vapor) for transmittance calculation come from JMA's GSM (Global Spectral Model) forecast GPV data ( $0.5^\circ \times 0.5^\circ$ ).

It should be noted that this algorithm is sensitive to cloud top height retrieval errors and transmittance errors (i.e., RTTOV and GSM forecast errors). Cloud top height accuracy also depends on that of RTTOV and GSM forecasts (Mouri et al. 2016).

For each  $16 \times 16$ -pixel array, CSR is calculated as the average brightness temperature of clear pixels for each band. The product also includes information on the percentage of clear pixels, the standard deviation of clear sky brightness temperatures, the latitude/longitude and satellite/solar zenith angles of the center of the segment, and land/sea flags (output in Fig. 1).

### 3.3. Comparison with the MTSAT CSR algorithm

For users of MTSAT CSR, Table 2 compares the MTSAT and Himawari-8 CSR algorithms.

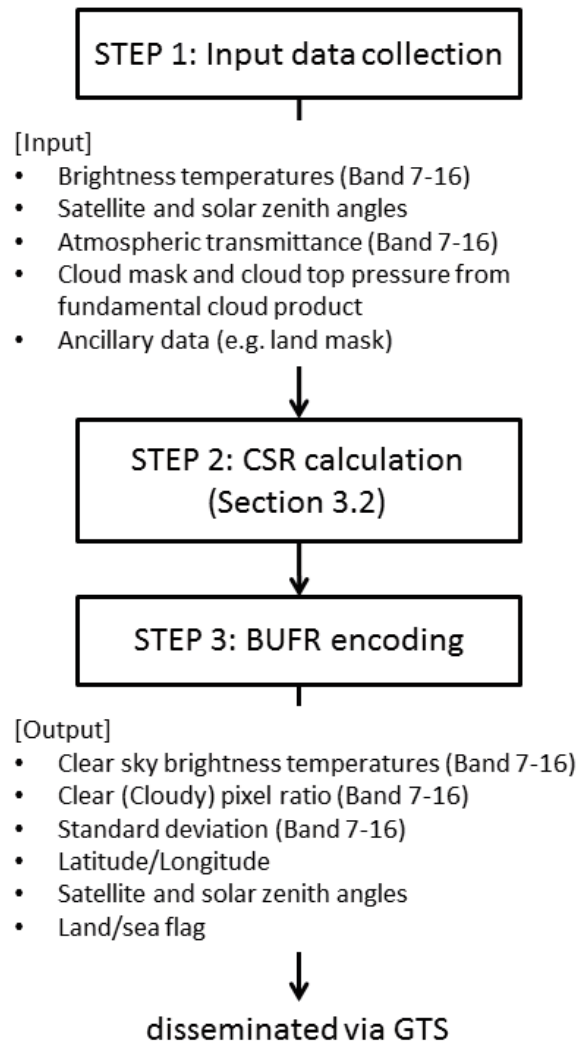


**Figure 1. Himawari-8 CSR processing**

For all 16 x 16 pixels in the segment

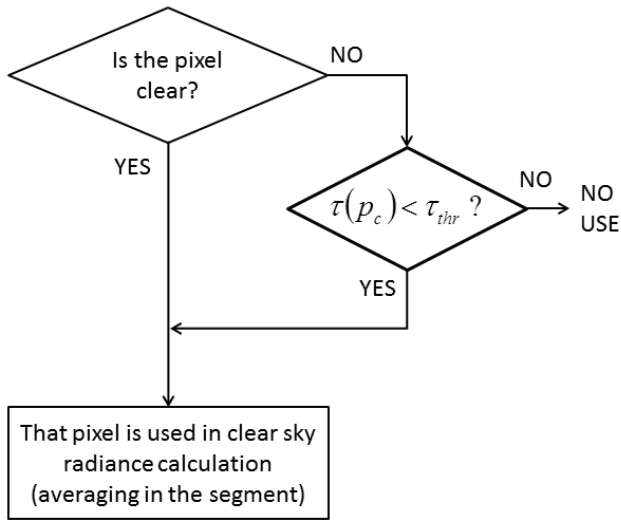


Figure 2. CSR calculation flowchart (see 3.2)

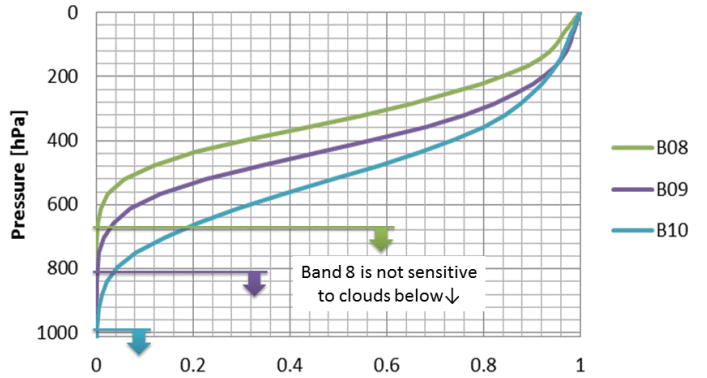


Figure 3. Atmospheric transmittances from pressure levels to TOA for AH1 bands 8, 9 and 10. The levels below which radiance from cloud is negligible differ for each band.

Table 2. Comparison of MTSAT and Himawari-8 CSR products

	MTSAT-CSR	Himawari-CSR
Segment size	16 x 16 IR-pixels (64 x 64 km at sub-satellite point)	16 x 16 IR-pixels (32 x 32 km at sub-satellite point)
Algorithm characteristics	Brightness temperatures of regular clear pixels (i.e., those with no cloud at any level) are averaged for CSR calculation. As a result, clear sky ratios for all bands are the same.	Cloudy pixels are regarded as clear in addition to regular clear pixels if the contribution of cloud top emission to the total radiance is negligible. This results in more data for WV bands than with the MTSAT-CSR algorithm, and clear pixel ratios differ for each band (see 3.2).
Reference	Uesawa (2009)	This document



#### 4. Results

Figure 4 shows the Himawari-8 CSR product for bands 8, 9, and 10 (i.e., water vapor bands) for 00 UTC on 15 August 2015. The clear pixel ratios differ for each band as expected from Fig. 3, which suggests that the number of clear pixels decreases in the order of bands 8, 9, and 10.

#### 5. Conclusions

MSC has routinely derived the CSR product from Himawari-8 full-disk observation data since 7 July 2015.

The spatial coverage extends to satellite zenith angles of  $65^\circ$  from the sub-satellite point. Processing is performed on an hourly basis (with full-disk observations from (hh-1):50 to hh:00). CSR is determined for each  $16 \times 16$  infrared pixel array, which corresponds to a resolution of  $32 \times 32 \text{ km}^2$  at the sub-satellite point. It should be noted that clear (cloudy) pixel ratios differ for each band (see Section 3.2). CSR data are encoded in BUFR format and distributed via the Global Telecommunication System (GTS). NWP centers will start to use the Himawari-8 CSR product in their operational assimilation systems after evaluation.

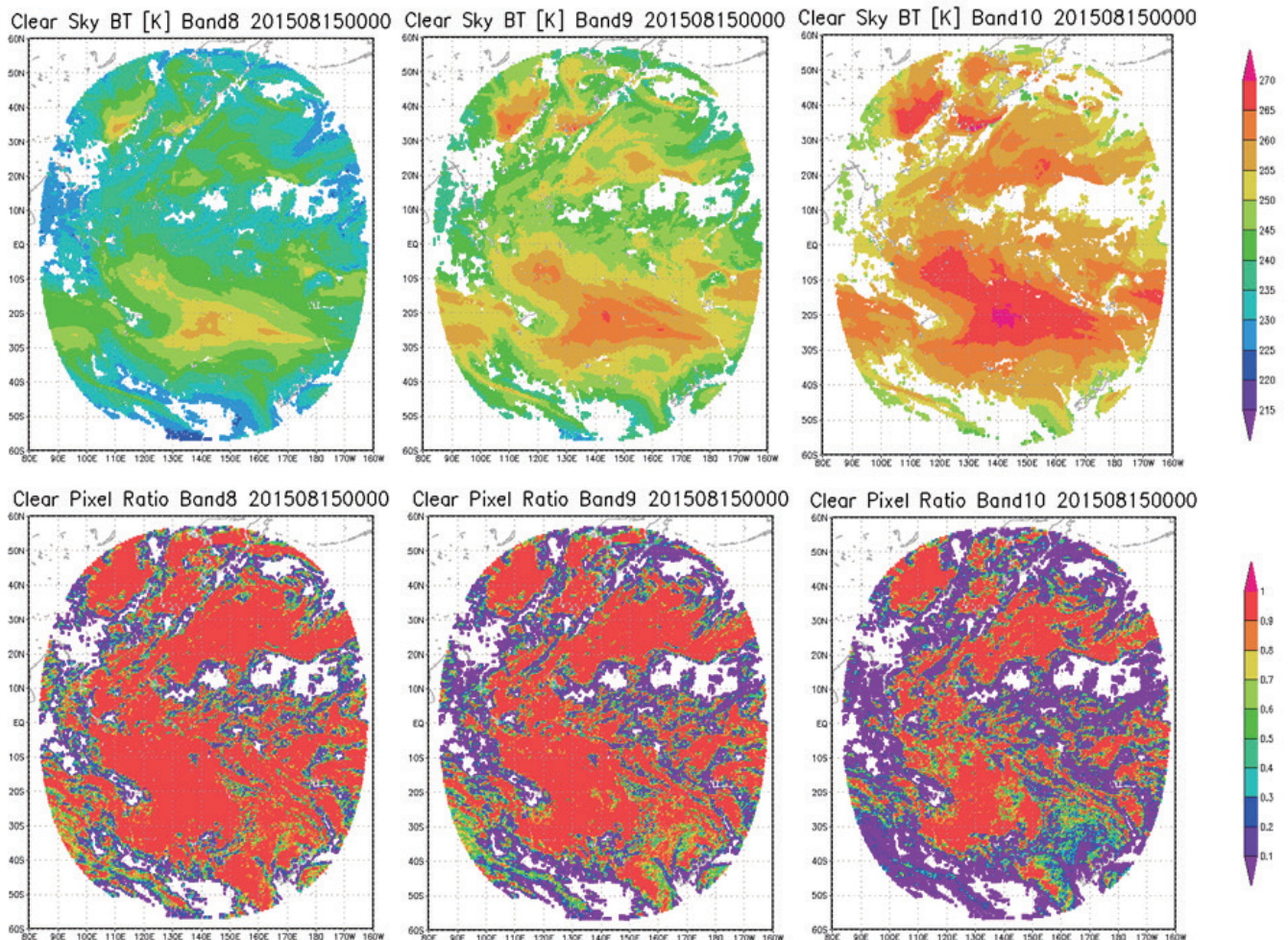


Figure 4. Himawari-8 CSR product for 00 UTC on 15 August 2015: clear sky brightness temperatures [unit: K] (top row) and clear pixel ratios (bottom row) for bands 8 ( $6.2 \mu\text{m}$ ; left), 9 ( $6.9 \mu\text{m}$ ; center), and 10 ( $7.3 \mu\text{m}$ ; right)

## References

- Bessho, K., K. Date, M. Hayashi, A. Ikeda, T. Imai, H. Inoue, Y. Kumagai, T. Miyakawa, H. Murata, T. Ohno, A. Okuyama, R. Oyama, Y. Sasaki, Y. Shimazu, K. Shimoji, Y. Sumida, M. Suzuki, H. Taniguchi, H. Tsuchiyama, D. Uesawa, H. Yokota, and R. Yoshida, 2016: An introduction to Himawari-8/9 - Japan's new-generation geostationary meteorological satellites. *J. Meteor. Soc. Japan*, 94, doi:10.2151/jmsj.2016-009.
- EUMETSAT, 2014: MSG Meteorological Products Extraction Facility Algorithm Specification Document (EUM/MSG/SPE/022, v7A, 20 March 2014) [Available online at [www.eumetsat.int/website/home/Data/TechnicalDocuments/index.html](http://www.eumetsat.int/website/home/Data/TechnicalDocuments/index.html) (Accessed 20 August 2015)]
- Eyre, J.R., 1991: A fast radiative transfer model for satellite sounding systems. *ECMWF Tech. Memo.* 176, 28pp
- Imai, T., and R. Yoshida, 2016: Algorithm theoretical basis for Himawari-8 Cloud Mask Product. *Meteorological Satellite Center Technical Note*, 61, 1-17.
- Matricardi, M., F. Chevallier, G. Kelly, and J.-N. Thépaut, 2004: An improved general fast radiative transfer model for assimilation of satellite radiance observations. *Quart. J. Roy. Meteor. Soc.*, 130, 153-173.
- Mouri, K., H. Suzue, R. Yoshida, and T. Izumi, 2016: Algorithm Theoretical Basis Document of Cloud top height product. *Meteorological Satellite Center Technical Note*, 61, 33-42.
- Saunders, R. W., M. Matricardi, and P. Brunel, 1999: An improved fast radiative transfer model for assimilation of satellite radiance observations. *Quart. J. Roy. Meteor. Soc.*, 125, 1407-1425.
- Uesawa, D., 2009: Clear Sky Radiance (CSR) product from MTSAT-1R. *Meteorological Satellite Center Technical Note*, 52, 39-48.

---

### ひまわり 8 号データによる晴天放射輝度温度プロダクト

今井 崇人\*、上澤 大作\*\*

#### 要 旨

気象衛星センターはひまわり 8 号晴天放射輝度温度プロダクト (CSR) を開発し、2015 年 7 月 7 日より数値予報センターへの提供を行なっている。CSR は晴天ピクセルの放射輝度や輝度温度の領域平均値を与えるデータである。雲のあるピクセルであっても、雲頂からの放射量が無視できるほど小さい場合は晴天とみなすことが可能であり、そのようなピクセルを晴天ピクセルとみなしてひまわり 8 号 CSR は算出される。ひまわり 8 号 CSR は 16×16 ピクセル単位 (赤道直下点で 32×32 km の分解能に相当) に含まれる晴天ピクセルの輝度温度の平均値を提供する。本プロダクトは数値予報モデルへの同化に利用される。

---

\* 気象庁観測部観測課観測システム運用室

\*\* 気象衛星センターデータ処理部システム管理課

# Aerosol Optical Depth product derived from Himawari-8 data for Asian dust monitoring

UESAWA Daisaku\*

## Abstract

The Meteorological Satellite Center (MSC) of the Japan Meteorological Agency (JMA) has developed an aerosol optical depth (AOD) product using visible and near-infrared Himawari-8 data collected during the daytime. The product is used in JMA's Asian dust monitoring.

## 1. Introduction

Aerosol optical depth (AOD) products based on satellite data are used by the Japan Meteorological Agency (JMA) to monitor dust events in East Asia. JMA's Meteorological Satellite Center (MSC) has derived AOD products from GMS-5 (Okawara et al. 2003) and from MTSAT-1R/-2 satellites (Hashimoto 2005).

A new AOD algorithm for Himawari-8 developed by JMA's Meteorological Research Institute (MRI) has also been incorporated into the MSC product server system.

This paper describes the Himawari-8 AOD product. The algorithm is outlined in Section 3.

## 2. Himawari-8

Himawari-8 is the world's first next-generation geostationary meteorological satellite (Bessho et al. 2016). It was launched on 7 October 2014 and has been operational since 7 July 2015. The unit took over East Asia and Western Pacific observation previously conducted for more than three decades by five GMS (geostationary meteorological satellite) units and two satellites from the MTSAT (multifunctional transport satellite) series.

Himawari-8 carries the Advanced Himawari Imager (AHI), which has 16 bands (See Table 1 for AHI specifications). Himawari-8/AHI performs full-disk observations at 10-minute intervals, and observes the Japan area and specific target areas at 2.5-minute

intervals. The Himawari-8 AOD product is derived from full-disk observations conducted during the daytime.

**Table 1. Himawari-8 AHI specifications**

	Band #	Central wavelength (μm)	Spatial resolution (km)
Visible	#1	0.47	1
	#2	0.51	
	#3	0.64	0.5
Near-infrared	#4	0.86	1
	#5	1.6	2
	#6	2.3	
Infrared	#7	3.9	
	#8	6.2	
	#9	6.9	
	#10	7.3	
	#11	8.6	
	#12	9.6	
	#13	10.4	
	#14	11.2	
	#15	12.4	
#16	13.3		

## 3. Algorithm

### 3.1. Overview

AOD (at 0.5 μm) and the Ångström exponent (a proxy for particle size) are simultaneously estimated for areas over the ocean using two bands with signals different to those of particle size. AOD (at 0.5 μm) is estimated for areas over land using the near-infrared band (2.3 μm) adopted for estimation of land surface (background) reflectance. Lookup tables (LUTs) representing

\* System Engineering Division, Data Processing Department, Meteorological Satellite Center

(Received August 28, 2015, Accepted November 20, 2015)



theoretical relationships between AHI visible and near-infrared reflectances and aerosol properties are compiled from radiative transfer simulation (see Section 3.2). AOD and the Ångström exponent are retrieved from the LUTs using Himawari-8 observation. As the aerosol type is assumed to be Asian dust for the LUTs, the algorithm is not optimized for other aerosol types (e.g., haze).

The processing of the algorithm is as outlined below. A flowchart of the processing is shown in Figure 1.

- Step 1 (input data collection): AOD product processing involves use of the data listed below. All data files are stored in a 5,500 x 5,500 infrared pixel array.
  - Radiances (bands 3, 4, 6)
  - Satellite/Solar zenith/Azimuth angles
  - Cloud mask from fundamental cloud product (Imai and Yoshida 2016)

Spatial coregistration is completed in such a way that a 4 x 4 pixel array for AHI band 3 (0.64  $\mu\text{m}$ ) and a 2 x 2 pixel array for band 4 (0.86  $\mu\text{m}$ ) nominally correspond to an infrared pixel (see Table 1 for the spatial resolution of each band). The radiances of bands 3 and 4 are spatially averaged.

Reflectance is defined as

$$R = \pi I / S_0 \cos(\theta_0),$$

where  $I$  is radiance,  $S_0$  is solar irradiance and  $\theta_0$  is the solar zenith angle. The reflectances of bands 3, 4 and 6 ( $R_{0.64}$ ,  $R_{0.86}$  and  $R_{2.3}$ ) are used in the subsequent steps.

- Step 2 (scene selection): AOD is retrieved for clear pixels during the daytime. Cloud mask comes from a fundamental cloud product (Imai and Yoshida 2016). Scenes with either of following are excluded from processing:
  - Sun glint angle (i.e., the angle between the satellite viewing direction and the direction of specular reflection)  $< 30^\circ$
  - Satellite/Solar zenith angles  $> 70^\circ$

Land and sea areas are differentiated using land mask data.

As aerosols cannot be detected over bright surfaces such as those of desert areas, only dark

scenes ( $R_{2.3} < 0.25$ ) are targeted for retrieval over land.

If  $(R_{0.86} - R_{2.3}) / (R_{0.86} + R_{2.3}) < 0.1$ , the land surface type is judged to be soil; otherwise, it is marked as vegetation. Different LUTs are used for each.

- Step 3 (LUT interpolation): As LUT data are functions of satellite-earth-sun geometry (i.e., satellite/solar zenith angles and relative azimuth angles), LUTs are interpolated to fit the geometry for each pixel.
- Step 4 (retrieval): AOD and the Ångström exponent are retrieved from the interpolated LUT using band 3 and 4 reflectances for areas over the ocean. AOD and the surface reflectance of band 6 are retrieved from the interpolated LUT using band 3 and 6 reflectances. The surface reflectance of band 3 is determined as a function of that of band 6 in the LUT.
- Step 5 (output): AOD and the Ångström exponent (over ocean areas only) are provided as GPV data ( $0.02^\circ \times 0.02^\circ$ ).

### 3.2. LUT calculation

LUTs are provided by Yuzo Mano of MRI. The settings of LUT calculation basically follow Mano et al. 2009.

- Aerosol model  
Bimodal log-normal size distribution is assumed. Aerosol particles are assumed to be spheroidal and randomly oriented. The minor/major-axis ratio is based on the study of Okada et al. 2001, in which mineral aerosols were sampled in arid regions of China and their particle shapes were examined using an electron microscope. The complex refractive index is essentially the same as that of Mano et al. 2009.
- Surface reflectance  
The ocean surface is simulated using multiple facets whose slopes vary with wind speed over the ocean (Cox and Munk 1954). A constant wind speed of 5 m/s is assumed.
- Radiative transfer model



The atmosphere is divided into two layers (1,013 – 500 hPa and 500 – 100 hPa). Each layer is assumed to be plane-parallel and vertically homogeneous. Aerosols are located in the lower layer. Radiative transfer is calculated using the discrete ordinate method with 150 streams.

Figure 2 shows examples of LUTs for AOD retrieval.

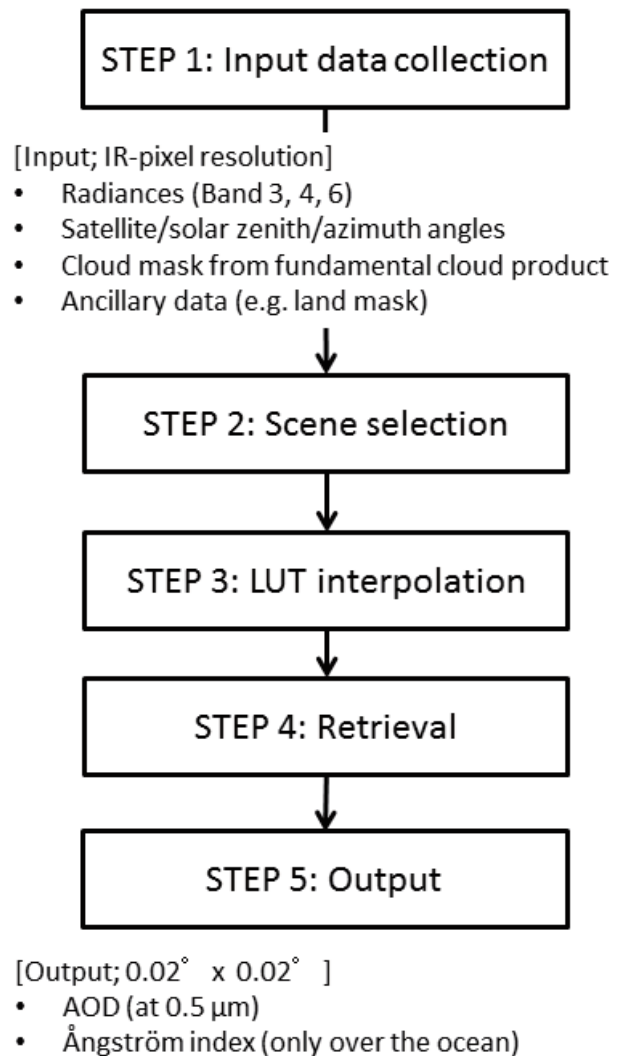
**4. Results**

Figure 3 shows the Himawari-8 AOD product for 00 UTC on 1 August 2015. The AOD values and distribution seem reasonable with reference to MSC’s MTSAT-2 AOD product and JMA’s sun-photometer AOD product. However, the distribution of the Ångström exponent (not shown) is questionable, and remains under investigation.

Another issue involves detection of thick aerosols, which are sometimes missing from the product. Figure 4 shows an example. With reference to other sources (e.g., MSC’s MTSAT-2 AOD product), the blank area surrounded by aerosols around 41°N appears to be thick aerosols. From this, it can be inferred that cloud mask tends to classify thick aerosol as cloud.

**5. Conclusion**

MSC has routinely derived the AOD product from Himawari-8 full-disk observation data since 7 July 2015. The spatial coverage is 114°E – 160°E, 52°N – 17°N. Processing is performed hourly during the daytime (full disk observations from (hh-1):50 to hh:00; hh = 00 – 06). The Himawari-8 AOD product is used for Asian dust monitoring by JMA.



**Figure 1. Himawari-8 AOD product processing**

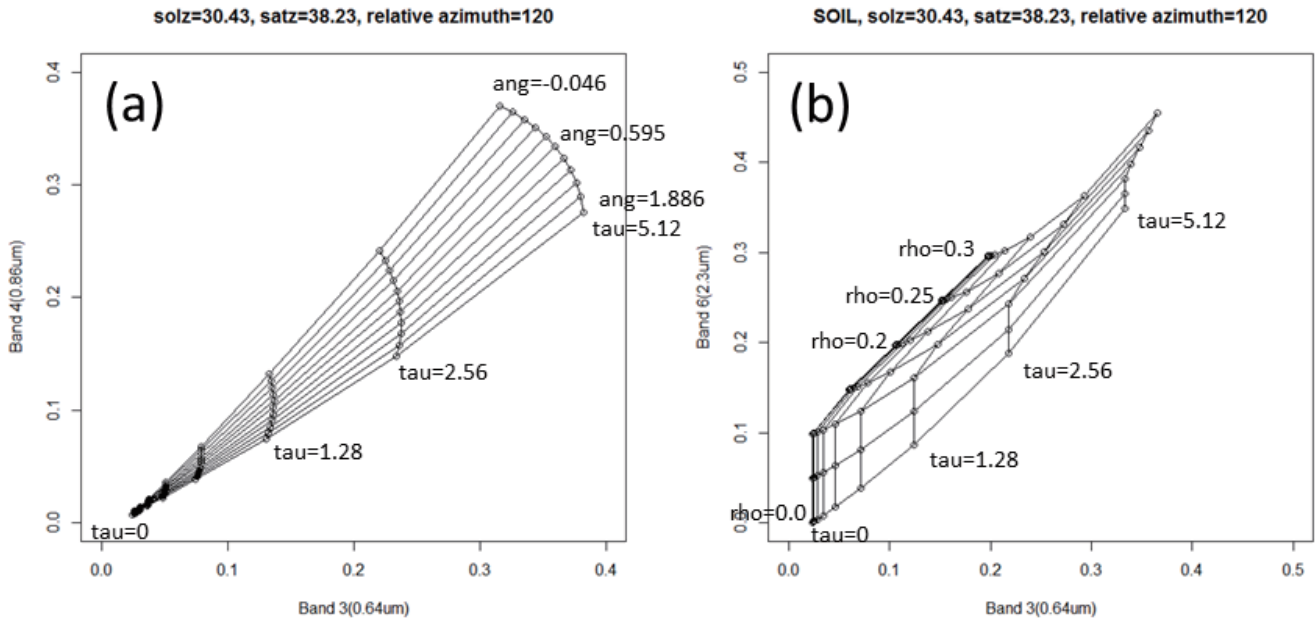


Figure 2. (a) Theoretical relationship between the reflectances of Himawari-8 AHI bands 3 and 4 over ocean areas for various aerosol loading conditions. AOD (denoted as tau) = 0.000, 0.020, 0.040, 0.080, 0.160, 0.320, 0.640, 1.280, 2.560 and 5.120; Angstrom index (denoted as ang) = 1.886, 1.529, 1.235, 0.988, 0.777, 0.595, 0.435, 0.294, 0.169, 0.056 and -0.046; solar zenith angle = 30.43°, satellite zenith angle = 38.23°, and relative azimuth angle = 120°. (b) Theoretical relationship between the reflectances of Himawari-8 AHI bands 3 and 6 over land areas (soil type) for various aerosol loading conditions. AOD (denoted as tau) = 0.000, 0.020, 0.040, 0.080, 0.160, 0.320, 0.640, 1.280, 2.560 and 5.120; surface reflectance of band 6 (denoted as rho) = 0.30, 0.25, 0.20, 0.15, 0.10, 0.05 and 0.00; solar zenith angle = 30.43°, satellite zenith angle = 38.23° and relative azimuth angle = 120°.

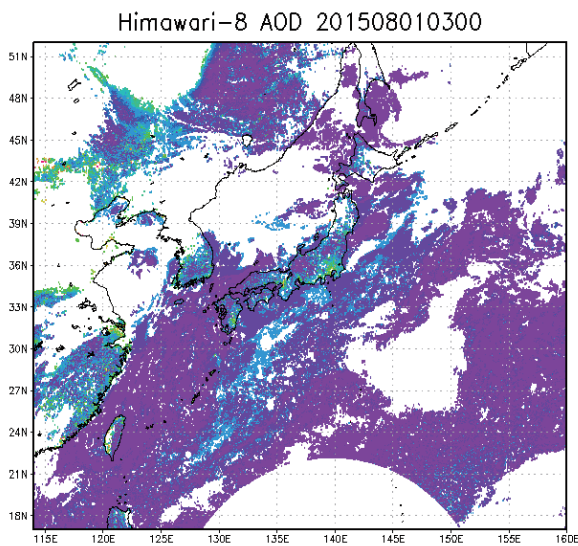


Figure 3. Himawari-8 AOD product for 00 UTC on 1 August 2015

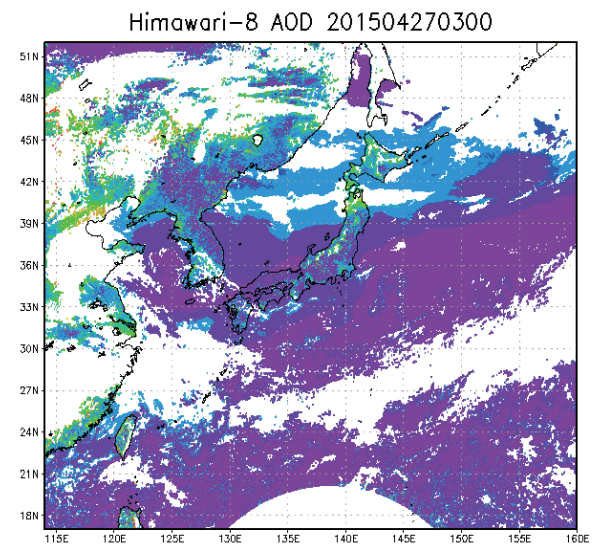


Figure 4. Himawari-8 AOD derived from in-orbit test data for 03 UTC on 27 April 2015

## References

- Bessho, K., K. Date, M. Hayashi, A. Ikeda, T. Imai, H. Inoue, Y. Kumagai, T. Miyakawa, H. Murata, T. Ohno, A. Okuyama, R. Oyama, Y. Sasaki, Y. Shimazu, K. Shimoji, Y. Sumida, M. Suzuki, H. Taniguchi, H. Tsuchiyama, D. Uesawa, H. Yokota, and R. Yoshida, 2016: An introduction to Himawari-8/9 - Japan's new-generation geostationary meteorological satellites. *J. Meteor. Soc. Japan*, 94, doi:10.2151/jmsj.2016-009.
- Cox, C., and W. Munk, 1954: Measurement of the roughness of the sea surface from photographs of the sun's glitter. *J. Opt. Soc. Am.*, 44, 838-850.
- Imai, T., and R. Yoshida, 2016: Algorithm theoretical basis for Himawari-8 Cloud Mask Product. *Meteorological Satellite Center Technical Note*, 61, 1-17.
- Hashimoto, T., 2005: Aerosol Optical Thickness. *Meteorological Satellite Center Technical Note*, Special Issue, 121-124. (in Japanese)
- Mano, Y., T. Hashimoto, and A. Okuyama, 2009: Verification of satellite-derived aerosol optical thickness over land with AERONET data. *Papers in Meteorology and Geophysics*, 60, 7-16.
- Okada, K., J. Heintzenberg, K. Kai, and Y. Qin, 2001: Shape of atmospheric mineral particles collected in three Chinese arid-regions, *Geophys. Res. Lett.*, 28, 3123-3126.
- Okawara, N., Y. Yoshizaki, and M. Tokuno, 2003: Development of Aerosol Products from GMS/VISSR and NOAA/AVHRR Image Data. *Meteorological Satellite Center Technical Note*, 42, 43-52. (in Japanese)

---

黄砂監視のためのひまわり 8 号エアロゾル光学的厚さプロダクト

上澤 大作\*

### 要 旨

気象衛星センターはひまわり 8 号エアロゾル光学的厚さ (AOD) プロダクトを開発した。AOD は可視・近赤外データを利用して日中算出される。本プロダクトは気象庁の黄砂監視業務で利用される。

---

\* 気象衛星センターデータ処理部システム管理課